The Sixteenth International Congress on Sound and Vibration
Kraków, 5-9 July 2009

VIBRATION ANALYSIS OF A MEMS RING-BASED RATE SENSOR BY THE RAY TRACING METHOD

Benjamin Chouvion, Stewart McWilliam, Colin Fox and Atanas Popov

University of Nottingham, University Park, Nottingham NG7 2RD, United Kingdom,
email: eaxbc@nottingham.ac.uk

In this paper a wave approach, known as the ray tracing method, is used to analyse the vibration performance of a Micro-Electro-Mechanical Systems (MEMS) ring-based rate sensor. This approach uses propagation and transmission of elastic waves, and fully exploits the presence of cyclic symmetry to determine the vibrating response. Sensor sensitivity is highly degraded by the presence of damping. Support loss is one of the important sources of damping in MEMS resonators and takes account of the energy dissipated through the supporting structure. Using classic wave theory in a two-dimensional thin plate, analytical expressions are obtained for substrate displacements due to shear and normal stresses being applied to its edge, and these displacements are used to determine the support loss. Numerical results for the natural frequencies and mode shapes of a MEMS ring-based rate sensor are provided and it is shown that they are in very good agreement with a finite element analysis. The corresponding support losses are also presented.

1. Introduction

The latest generation of vibrating rate sensors are manufactured using Micro-Electro-Mechanical Systems (MEMS) technology and are designed to have high mechanical quality factors (Q). The Q-factor is a measure of damping and governs the performance (sensitivity and accuracy) of the rate sensor. Support loss is one important damping mechanism for MEMS rate sensors, and governs the losses from the resonator to its foundation through the supporting structure. Support loss induced by the vibrational displacement of the foundation (substrate) due to stress sources arising from the resonator has been studied previously in [1–3]. In this paper, the support model approach of [1] is applied to the rate sensor shown in Fig. 1, which consists of a slender circular ring supported on slender legs.

A wave approach can be used to efficiently model the vibrations of coupled ring/beam structures like that shown in Fig. 1. This approach is used here to determine the natural frequencies and mode shapes [4] and the energy transmitted through the structure – the latter being used as a basis for calculating the support loss.

The vibrations of elastic structures, such as coupled ring/beam components, can be described in terms of waves that propagate and decay in waveguides. Langley [5] developed a ray tracing method to evaluate the response of one-dimensional structures subjected to harmonic excitation. This method has been extended to the study of straight and curved beam structures, and to include near-field wave components, in [4], and is used here to analyse the rate sensor shown in Fig. 1.

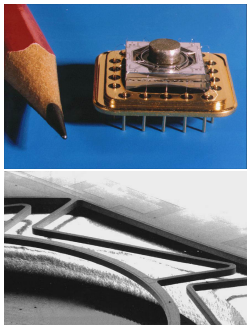

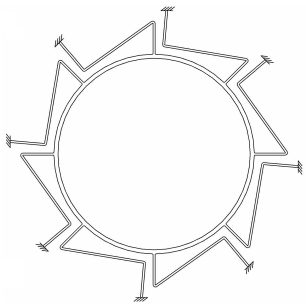

Figure 1. Photographs and schematic representation of the ring-based rate sensor and its leg shape

The ultimate aim of the research is to determine the Q-factor associated with the support loss of the rate sensor. The Q-factor is defined by:

$$Q = 2\pi \frac{W}{\Delta W} \tag{1}$$

where W denotes the maximum vibration energy stored per cycle of vibration and ΔW is the energy dissipated per cycle. In this work, the ray tracing method (Section 2) is used to determine the mode shapes of the sensor and then calculate the W-term – i.e. the overall strain energy of the sensor. The ray tracing approach is also used to determine the stresses at the "clamped" interface between the supporting structure and the foundation (substrate). These results are combined with the support loss model [1] presented in Section 3, to obtain ΔW in Eq. (1). Section 4 presents numerical results for the natural frequencies and Q-factors for different modes of vibration of the sensor illustrated in Fig. 1.

2. Ray tracing method

The ray tracing method is similar to the phase or wave-train closure principle [6]. It provides a straightforward and efficient way to calculate the natural frequencies and modes shapes of structures composed of waveguides. It has been applied previously to Timoshenko beams [7] and curved beams [8], and is applied here to a coupled ring/beam structure.

2.1 Displacements definition

The ray tracing method is a "wave approach" that models the different components of the structure as waveguides. In each component, the displacements are defined as a sum of propagating far-field and decaying waves [8, 9], that propagate and decay in each direction – the influence of damping is neglected here. Flexural and longitudinal waves for a straight beam, or radial and tangential waves for a curved beam, are present and travel (propagate and decay) in each direction. Each wave amplitude is associated with a particular wavenumber. These wavenumbers are obtained by solving the characteristic (dispersion) relation for the wavenumbers in straight [9] or curved [8] beams. In a curved beam component, the radial and tangential displacements are coupled. The number of unknown wave amplitudes per straight/curved waveguide component is always equal to six.

The main purpose of the ray tracing method is to relate the complex wave amplitudes of the different wave types within the structure at a particular frequency, and to achieve this it is necessary to understand the coupling between waves in neighbouring components using transmission coefficients.

2.2 Development of the ray tracing method

The displacements in each component of the structure are represented as a sum of waves. As the waves travel from one end of a component (j) to the other, the propagating waves change phase

and the decaying waves change amplitude. These effects are governed by the wavenumber k_p (where p is the type of wave; $k_p = k_L$, k_F and $-ik_F$ for straight beams: k_L and k_F being the longitudinal and flexural wavenumbers in beams [9]; $k_p = k_1$, k_2 and k_3 for curved beams [8]); and the length $L^{(j)}$ of the component. As the waves travel, the complex amplitude of the waves change from $\hat{u}_p^{(j)}$ to $\hat{u}_p^{(j)}\, e^{-ik_pL^{(j)}}$. For the purposes of analysis it is convenient to define a vector $\mathbf{a}$ whose p^{th} element $\hat{u}_p$ contains the p^{th} wave amplitude, and a diagonal matrix $\mathbf{D}$ called the dispersion matrix (or transfer matrix in [7]) whose p^{th} diagonal element is $\mathrm{D}_{pp} = e^{-ik_pL^{(j)}}$.

When a wave reaches the end of the component, it impinges on a joint (i.e. an external boundary or interface between components), and it is either reflected back in the opposite direction or transmitted to the neighbouring components. By considering the complex wave amplitude transmission/reflection coefficients, the amplitude of the waves leaving the joint in each component can be evaluated. For the purposes of analysis it is convenient to express this using a transmission matrix $\mathbf{T}$ containing complex wave amplitude transmission/reflection coefficients, where $\hat{u}_i = \mathrm{T}_{ij}\hat{u}_j$ and T_{ij} is the transmission/reflection coefficient from wave j to wave i. With 6 waves per component (3 propagating in each direction), the dimension of the matrices $\mathbf{T}$ and $\mathbf{D}$ is $6n \times 6n$, where n is the total number of components.

If the structure is vibrating freely in an undamped mode, the ray tracing method [5] stipulates that the wave amplitudes defining the displacement of the complete structure are the same as the wave amplitudes after the waves have performed one ray trace (i.e. propagated across each component and transmitted across a joint to a neighbouring element), i.e.

$$\mathbf{a} = \mathbf{TD}\,\mathbf{a}. \tag{2}$$

The natural frequencies of the system can be calculated by solving

$$\left|\mathbf{I} - \mathbf{TD}\right| = 0 \tag{3}$$

where $\mathbf{I}$ is the $6n \times 6n$ identity matrix.

2.3 Transmission coefficients

In general, the transmission coefficients are calculated by considering the continuity and force equilibrium equations at each joint, with the joint being taken in isolation from the rest of the structure. It is necessary to calculate the transmission coefficients arising, from each wave type impinging on a junction to all waves types in all neighbouring components. For a joint having n components, the force and moment equilibrium as well as displacement and slope continuity equations provide a total of $3n$ equations in terms of $3n$ unknown transmission coefficients. Solving these equations yields the transmission coefficients, which are then used in the transmission matrix $\mathbf{T}$.

For the rate sensor shown in Fig. 1, it will be necessary to consider leg boundaries (clamped), two angled beam joints, and T-joints between a ring and an attached beam. For the external boundaries, $n = 1$ and the transmission/reflection coefficients are obtained by solving 3 equations. For the two beam joints, $n = 2$ and the transmission coefficients are obtained by solving the resulting 6 equations. For the T-joints, $n = 3$ and the transmission coefficients are obtained by solving the resulting 9 equations. If identical joints occur within a structure, the transmission coefficients only need to be calculated once.

2.4 Simplification using cyclic symmetry

Thomas [10] developed a simplification for cyclic (or rotational) symmetric structures, $360°$ structure that consists of repetitive sectors, for use with the Finite Element (FE) method, and this method can be applied easily to the ray tracing method [4]. The basic idea is that the displacements

for any sector can be related to the displacements of just one particular sector by a phase angle ψ. The sectors are numbered sequentially (j) (with $j = 1, \ldots, N$), increasing in the positive direction of propagation (assumed to be clockwise). In the context of the wave approach the wave amplitudes $\mathbf{a}^{(j)}$ for the j^{th} sector and the wave amplitudes $\mathbf{a}^{(j+1)}$ for the $(j+1)^{\text{th}}$ sector are linked as follows

$$\mathbf{a}^{(j)} = e^{-i\psi}\,\mathbf{a}^{(j+1)} \tag{4}$$

where $\psi = 2\pi\kappa/N$, N is the total number of identical sectors, and κ is the number of nodal-diameters. This equation represents a phase change of ψ (or $-\psi$) between one end of a sector and its other end. κ can take the following values [10] $\kappa = 0,\ 1,\ \ldots,\ N/2$ (N even) or $\kappa = 0,\ 1,\ \ldots,\ (N+1)/2$ (N odd). Each value corresponds to a κ-fold symmetric mode and each mode must be examined independently.

The ring-based rate sensor illustrated in Fig. 1 has cyclic symmetry, and each one of the eight ($N = 8$) sectors contains one leg (composed of 3 straight beams) and a $45°$ ring portion. The principal sector of this type of sensor is shown in Fig. 2 (a); while Fig. 2 (b) shows its typical dimensions.

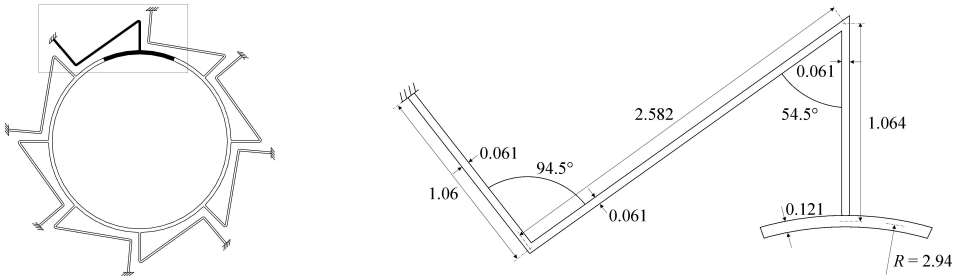

(a) (b)

Figure 2. (a) Ring-based rate sensor with cyclic symmetry and its $45°$ principal sector; (b) Actual modelled structure and its dimensions in mm (with axial thickness $= 0.1$ mm)

In the ray tracing method, only the principal sector is modelled. The phase change ψ appearing in Eq. (4) is represented as a "transmission coefficient" from one end of the sector to the other. If the complex displacement at its left end is u, then the displacement at its right end will be $u\,e^{-i\psi}$. Correspondingly, if its displacement is u at its right end, then it will be $u\,e^{i\psi}$ at its left end. Thus, the waves incident on one end and the waves transmitted to the other end will have an amplitude ratio of $e^{-i\psi}$ (or $e^{i\psi}$). The transmission matrix $\mathbf{T}$ of Eq. (3) will contain, in addition to the transmission coefficients from the joints, terms in $e^{-i\psi}$ and $e^{i\psi}$ that represent this particular cyclic symmetry "transmission".

3. Support loss model

3.1 Physical modelling and main assumptions

A MEMS resonator must be attached to a foundation (or substrate). This attachment can take different forms but typically the resonator and substrate are etched in the same plane, from the same silicon wafer. The joint interface between the resonator and substrate, which is often modelled as being clamped, is subjected to time-harmonic stresses that excite elastic waves in the substrate. These waves propagate into the substrate and carry energy away from the resonator. In this way the support structure absorbs some of the vibration energy from the resonator.

For a simple cantilever beam resonator [1], the support interface is subjected to time-harmonic stresses due to shear stress only. However, in more complex resonators such as the one shown in Fig. 1, the supporting legs produce both shear and tensile stresses simultaneously, see Fig. 3.

It has been shown [3] that a MEMS resonator and its substrate can reasonably be analysed separately. Based on the significant dimensional difference between a typical resonator and its substrate, it can be assumed that all the energy entering the support propagates away to large distances and no

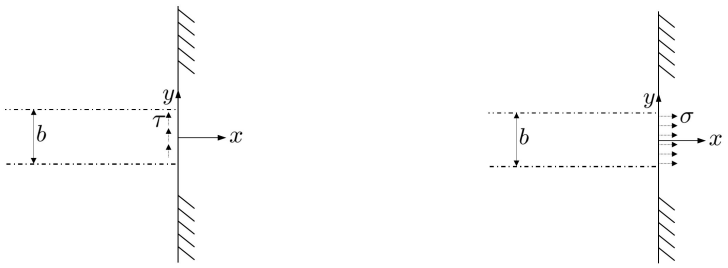

Figure 3. Semi-infinite thine plate with excitation sources, (a) Shear stress; (b) Normal stress

energy returns to the resonator. The support is modelled as being semi-infinite, and ensures that the calculated support loss is an upper bound of the actual support loss. For the sensor shown in Fig. 1, the resonator and its substrate lie in the same plane, and all the vibrations occur in plane. Assuming that the thickness (h) of the resonator is much smaller than the wavelength of the elastic waves propagating in the support, the substrate is modelled as a 2D thin plate undergoing plane stress.

A theoretical derivation of the vibrational displacement of the substrate is possible if it is assumed that the stress source is uniformly distributed across the clamped interface region.

3.2 Main steps of the derivation of vibration displacements of the substrate

This derivation follows the work done in [1], with the difference that shear and normal stresses act on the substrate at the same time. The vibration of the resonator causes elastic waves to propagate into the support. These waves are analysed using 2D elastic wave theory for the in-plane displacements [9]:

$$\frac{\partial^2 u}{\partial t^2} = c_L^2 \frac{\partial^2 u}{\partial x^2} + c_T^2 \frac{\partial^2 u}{\partial y^2} + \left(c_L^2 - c_T^2\right) \frac{\partial^2 v}{\partial x \partial y} \tag{5a}$$

$$\frac{\partial^2 v}{\partial t^2} = c_L^2 \frac{\partial^2 v}{\partial y^2} + c_T^2 \frac{\partial^2 v}{\partial x^2} + \left(c_L^2 - c_T^2\right) \frac{\partial^2 u}{\partial x \partial y} \tag{5b}$$

where u and v are the displacements in the support along the x- and y- axes, respectively, and c_L and c_T are the propagation velocities for longitudinal and transverse waves, respectively. It is assumed that these displacements are time-dependant at frequency ω (excitation frequency) and have the form $u = \hat{u}\, e^{-i\omega t}$ and $v = \hat{v}\, e^{-i\omega t}$.

Shear stress τ acting parallel to the y-axis and normal stress σ acting parallel to the x-axis are generated by the vibration of the sensor and are given by the stress-strain relationships for a thin plate [9]:

$$\tau = \rho c_T^2 \left(\frac{\partial \hat{u}}{\partial y} + \frac{\partial \hat{v}}{\partial x} \right) \tag{6a}$$

$$\sigma = \rho c_L^2 \frac{\partial \hat{u}}{\partial x} + \rho \left(c_L^2 - 2c_T^2\right) \frac{\partial \hat{v}}{\partial y} \tag{6b}$$

where ρ is the mass density.

With the introduction of new operators (such as the divergence) that consider the cross-derivatives of $\hat{u}$ and $\hat{v}$ with respect to x and y, Eqs. (5) and (6) can be simplified so that no second order derivatives appear. To remove the double dependency in x and y, a Fourier transform is then applied to the new set of equations.

The system of 4 equations (Eqs. (5) and (6)) with 4 unknowns (the Fourier transform of $\hat{u}$, $\hat{v}$, τ, σ) can be solved by applying appropriate boundary conditions to remove any integration constants. The boundary conditions correspond to the stress (shear and normal) sources on the edge of the thin

plate (in $x = 0$) and are a function of the type of vibration induced by the resonator, see Fig. 3. For $\left|y\right| > b/2$, there is no stress source so $\sigma = \tau = 0$. Over the source region $\left|y\right| < b/2$ (width b of the clamped beam):

- for flexural vibrations: the shear stress is constant and the normal stress is linearly dependant of the y value (due to the bending moment);
- for longitudinal vibrations: the shear stress is 0 and the normal stress is constant.

The flexural and longitudinal displacements have now been derived in the Fourier domain for the two types of incident vibrations. The inverse Fourier transform is applied to obtain the solutions in the real domain and the displacements can be calculated at any point in the support. For instance, if only shear stresses due to a shear force F are considered and the support structure has the following material properties: Poisson's ratio $\nu = 0.28$, mass density $\rho = 2330\,\mathrm{kg/m^3}$ and Young's modulus $E = 170\,\mathrm{Gpa}$, the imaginary part of the flexural displacement induced at the support free edge is [1]:

$$\bar{v}_{x=0} = \frac{0.33505\, c_L^2\, F}{\pi \rho c_T^4 h} \tag{7}$$

This displacement is an average along the entire width b of the resonator and can be derived using the above procedure.

The amount of energy loss per cycle from the support can be calculated explicitly as:

$$\Delta W = \pi F \bar{u}_{x=0} \tag{8}$$

where F is the force producing the stresses τ or σ and $\bar{u}_{x=0}$ is the imaginary part of the induced displacement at the thin plate edge. Substituting the appropriate value of the average displacement (for instance Eq. (7)) in Eq. (8) the energy loss can be calculated. The support loss can then be derived using Eq. (1).

4. Results

The ray tracing method presented in Section 2 has been applied to the MEMS ring-based rate sensor illustrated in Fig. 1. The boundary conditions between the sensor and its substrate are considered to be clamped. The dimensions used are given in Fig. 2 (b). The sensor is modelled taking into account the cyclic symmetry properties of the structure (Section 2.4). As a result, only one leg (3 beam portions) and a 45° portion of the ring is modelled. To obtain all the natural frequencies of the sensor, five different analyses ($\kappa = 0,\ 1,\ 2,\ 3,\ 4$ see Section 2.4) are performed. For each κ, Eq. (3) is solved to calculate the natural frequencies of the sensor. The obtained natural frequencies are compared with FE models using Euler/Bernoulli or Timoshenko 2D beam elements in Table 1. The results are in excellent agreement (up to 5 significant figures) when Euler/Bernoulli elements are used. When Timoshenko elements are used, the percentage difference is less than 0.5%. This difference occurs because the ray tracing approach neglects shear deformation and rotatory inertia effect.

The mode shapes of the principal sector are calculated using the ray tracing method with cyclic symmetry simplification. As explained in Section 2.4, the mode shapes for all sectors can be obtained from the principal sector. The mode shapes of the complete sensor are then constructed. Mode shapes obtained using the FE and ray tracing methods are in excellent agreement.

The overall strain energy and stresses acting at the clamped ends can be calculated for each method, using the obtained mode shapes results. These quantities are used in the support loss model presented in Section 3. The vibration displacements of the substrate are a direct function of the time-harmonic stresses at the clamped ends and can also be calculated. From Eq. (1), the Q-factor

Table 1. Natural frequencies (Hz) for the ring-based rate sensor calculated using the ray tracing method and FE models (2D Euler/Bernoulli and Timoshenko beam elements). The ring dimensions are presented in Figure 2 (b). The material properties used are $\rho = 2330\,\mathrm{kg/m^3}$, $E = 170 \cdot 10^9\,\mathrm{N/m^2}$ and $\nu = 0$.

	Ray Tracing	FE analysis		Diff. %
		Euler beams	Timoshenko beams	
$\kappa = 0$	18 330	18 330	18 277	0.29
	40 787	40 787	40 725	0.15
	67 320	67 320	67 028	0.43
$\kappa = 1$	11 853	11 853	11 820	0.28
	38 479	38 479	38 416	0.16
	65 971	65 971	65 697	0.42
$\kappa = 2$	14 234	14 234	14 217	0.12
	37 850	37 850	37 784	0.17
	65 520	65 520	65 253	0.41
$\kappa = 3$	32 133	32 133	32 076	0.17
	41 100	41 100	41 001	0.24
	66 135	66 135	65 871	0.40
$\kappa = 4$	35 646	35 646	35 591	0.15
	55 202	55 202	54 978	0.41
	73 110	73 110	72 830	0.38

is derived using the FE and ray tracing methods. From the cyclic symmetry of the structure, two degenerate orthogonal mode pairs occur for each $\kappa = 1,\ 2,\ 3$, while for $\kappa = 0,\ 4$ modes do not occur in pairs. Fig. 4 presents the sensor mode shape of the lowest mode (and its orthogonal complement) for $\kappa = 0,\ 1,\ 2,\ 3,\ 4$ and the associated Q-factor calculated.

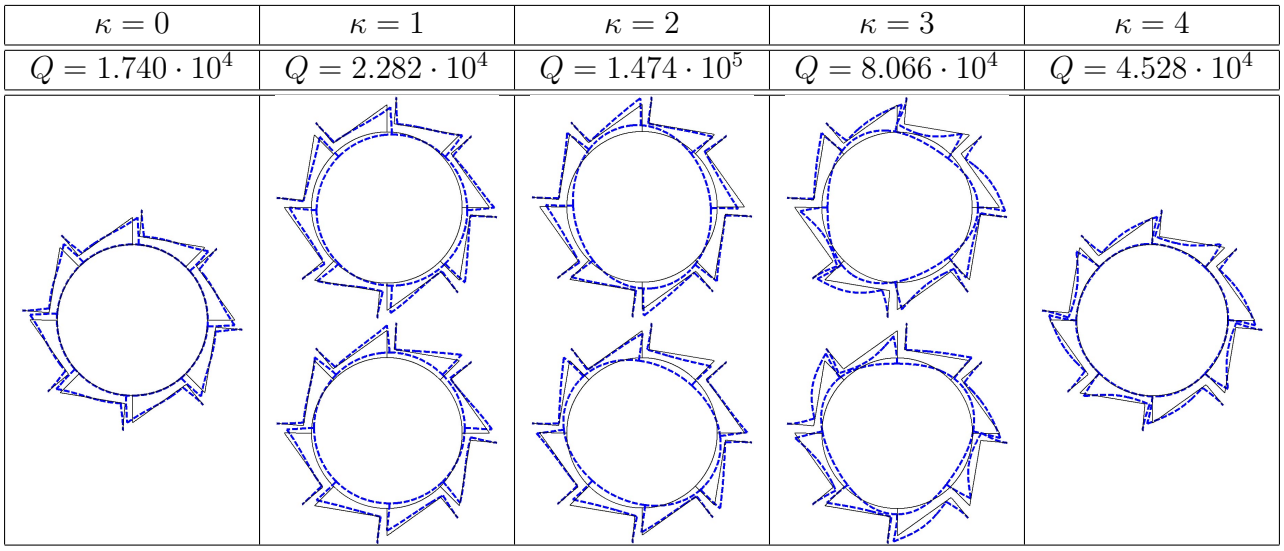

Figure 4. Mode shapes and calculated Q-factors of the ring-based rate sensor for the lowest natural frequency of each value of κ.

5. Conclusion

In this paper, a systematic approach, based on wave propagation is presented to study the free vibration of a MEMS rate sensor consisting of ring/beam elements. This ray tracing method was found to yield accurate and efficient predictions of the natural frequencies and mode shapes compared to the FE method. The resonator is connected to a foundation and the influence of the resonator on the

foundation is to provide stress sources that excite structural waves in the foundation. Modelling the foundation as a semi-infinite thin plate, an analytical expression for the displacement in the foundation due to a stress source was developed taking into account the normal and shear stresses simultaneously. This analysis together with the results obtained from a ray tracing analysis is used to calculate the support losses. Results for the support loss were obtained using this approach in conjunction with the ray tracing and FE methods. The results obtained were found to be in excellent agreement. It is worth noting that the same (approximate) support model is used throughout the paper, and that no attempt was made to validate this model. Future work aims to validate the support model used – one potential approach to achieve this is described in [11] and uses the FE method with semi-infinite elements. Once this has been achieved, the work will address the practical issue of designing the shape of the resonator to minimize the support loss.

Acknowledgements

The authors gratefully acknowledge the support of Atlantic Inertial Systems for this work.

References

[1] Z. Hao, A. Erbil, and F. Ayazi. An analytical model for support loss in micromachined beam resonators with in-plane flexural vibrations. *Sensors and Actuators A*, **109**, 156–164, 2003.

[2] D. M. Photiadis and J. A. Judge. Attachment losses of high Q oscillators. *Applied Physics Letters*, **85**(3), 482–484, 2004.

[3] M. C. Cross and R. Lifshitz. Elastic wave transmission at an abrupt junction in a thin plate with application to heat transport and vibrations in mesoscopic systems. *Physical Review B*, **64**, 1–22, 2001.

[4] B. Chouvion, S. McWilliam, C. H. J. Fox, and A. A. Popov. In-plane vibration analysis of ring/beam structures by wave propagation. *Journal of Sound and Vibration*. (in submission).

[5] R. S. Langley. High frequency vibration of one-dimensional systems: ray tracing, statistical energy analysis and vibration localisation, 1996. Private communication.

[6] L. Cremer, M. Heckl, and E. E. Ungar. *Structure-Borne Sound*. Springer-Verlag, Second edition, Berlin, 1988.

[7] C. Mei and B. R. Mace. Wave reflection and and transmission in Timoshenko beams and wave analysis of Timoshenko beam structures. *Journal of Sound and Vibration*, **127**(4), 382–394, 2005.

[8] B. Kang, C. H. Riedel, and C. A. Tan. Free vibration analysis of planar curved beams by wave propagation. *Journal of Sound and Vibration*, **171**, 695–702, 2005.

[9] K. F. Graff. *Wave Motion in Elastic Solids*. Ohio State University Press, 1975.

[10] D. L. Thomas. Dynamics of rotationally periodic structures. *International Journal for Numerical Methods in Engineering*, **14**, 81–102, 1979.

[11] M. Pandey. *Analysis of entrainment and clamping loss in an optically actuated MEMS*. Ph.D. thesis, Cornell University, 2008.